

Ideas about a pitch control system for the VIRYA-15 windmill ($\lambda_d = 8$, Gö 711 airfoil)

ing. A. Kragten

February 2010

KD 437

It is allowed to copy this report for private use.

Engineering office Kragten Design
Populierenlaan 51
5492 SG Sint-Oedenrode
The Netherlands
telephone: +31 413 475770
e-mail: info@dkwindturbines.nl
website: www.kdwindturbines.nl

Contains	page
1 Introduction	3
2 Description of the rotor of the VIRYA-15 windmill	3
3 Calculations of the rotor geometry	4
4 Determination of the C_p - λ and the C_q - λ curves	5
5 Determination of the P-n curves and the optimum cubic line	7
6 General aspects of pitch control systems	8
7 Choices made for the pitch control system of the VIRYA-15	10
8 Determination of the aerodynamic moment	11
9 Description of the synchronisation mechanism	14
10 Determination of the friction moment for Permaglide blade shaft bearings	16
11 Use of needle bearings for the blade shaft	17
12 Estimation of the braking capacity of the PM-generator	18
13 Functioning of the system for $V > 10$ m/s	21
14 References	22
fig. 7 Sketch synchronisation mechanism	23

1 Introduction

The VIRYA-15 windmill is designed for use in western countries as well as in developing countries. The windmill is meant to be connected to a 380 V or 400 V, 3-phase grid. The windmill has a simple two bladed rotor with wooden blades. In the first instance it is chosen to use a direct drive permanent magnet (PM) generator but it might be that the generator is driven by an accelerating gear box. The 3-phase generator current is rectified and the generated power is feed in the grid by an inverter.

The rotor has blades with a constant chord and airfoil and no blade twist which simplifies manufacture. The head is turned in the wind by an electric yawing motor which is steered by a wind vane. This system will have some slackening to prevent that the motor turns too often. The yawing motor can also be used to turn the rotor out of the wind.

The tower may be derived from the free standing 3-legs tower of the VIRYA-4.2 but will have a height of 24 m and is built up from four 6 m sections. The tower is provided with hinges at the tower foot and the whole windmill can be lifted by means of an auxiliary pole and a hoisting cable and winch.

The rotor will be equipped with a pitch control system which will be activated at a wind speed of 10 m/s. The pitch control system will be activated by the aerodynamic moment which is working on the airfoil. The chosen system will be described in chapter 7 and more.

2 Description of the rotor of the VIRYA-15 windmill

The 2-bladed rotor of the VIRYA-15 windmill has a diameter $D = 15$ m and a design tip speed ratio $\lambda_d = 8$. The most important advantages of a 2-bladed rotor above a 3-bladed rotor are that the connection of the blades to the hub is simple, that balancing of the rotor is rather simple and that the rotor can even be transported completely mounted.

The rotor has blades with a constant chord and blade angle and is provided with a Gö 711 airfoil. The geometry and characteristics of the Gö 711 airfoil are given in report KD 285 (ref. 1). The Gö 711 airfoil has only been measured for a Reynolds value of $4 \cdot 10^5$ but it is assumed that the characteristics can also be used for higher values. The maximum thickness is 14.85 % of the chord. The lower side of the Gö 711 airfoil is flat over 97.5 % of the chord which simplifies manufacture. It has a high maximum lift coefficient ($C_{l \max} = 1.5$ for $\alpha = 12.5^\circ$) and a low minimum drag-lift ratio ($C_d/C_l = 0.015$ for $C_l = 0.97$ and $\alpha = 3.7^\circ$).

A blade is made out of an about 7.1 m long planed hard wood plank with a width of 600 mm and a thickness of 90 mm. The plank can be built up from several strips which are glued together. The convex side of the airfoil is made by a rotating cutter with the shape of the airfoil in it. The airfoil is machined only over the outer 6.5 m of the blade length. The inner 0.6 m of the blade has a rectangular shape (with two bevelled edges, see figure 4) for connection of the blade to the pitch control mechanism. A blade is clamped in between two strips and is connected to the pitch control mechanism by three M24 bolts.

The blades will be rather flexible and therefore vibrations which are caused by the gyroscopic moment, by streaming under a certain yaw angle δ and by a non-uniform distribution of the wind speed over the rotor plane, are flattened. The distance in between the blade tip and the tower must be rather large to prevent that the blade tip may touch the tower during heavy wind gusts. The rotor shaft will therefore make a tilting angle of at least 5° with the horizon. The rotor is balanced by shortening the heaviest blade tip or by gluing small cylinders of lead in holes which are drilled in the blade tip.

3 Calculation of the rotor geometry

The rotor geometry is determined using the method and the formulas as given in report KD 35 (ref. 2). This report (KD 437) has its own formula numbering. Substitution of $\lambda_d = 8$ and $R = 7.5$ m in formula (5.1) of KD 35 gives:

$$\lambda_{rd} = 1.0667 * r \quad (-) \quad (1)$$

Formula's (5.2) and (5.3) of KD 35 stay the same so:

$$\beta = \phi - \alpha \quad (^\circ) \quad (2)$$

$$\phi = 2/3 \arctan 1 / \lambda_{rd} \quad (^\circ) \quad (3)$$

Substitution of $B = 2$ and $c = 0.6$ m in formula (5.4) of KD 35 gives:

$$C_l = 20.944 r (1 - \cos\phi) \quad (-) \quad (4)$$

Substitution of $V = 4$ m/s and $c = 0.6$ m in formula (5.5) of KD 35 gives:

$$Re_r = 1.60 * 10^5 * \sqrt{(\lambda_{rd}^2 + 4/9)} \quad (-) \quad (5)$$

The blade is calculated for fourteen stations A till N which have a distance of 0.5 m of one to another. The blade has a constant chord and the calculations therefore correspond with the example as given in chapter 5.4.2 of KD 35. This means that the blade is designed with a low lift coefficient at the tip and with a high lift coefficient at the root. First the theoretical values are determined for C_l , α and β . Next β is linearised such that the twist is constant and that the linearised values for the outer part of the blade correspond as good as possible with the theoretical values. The result of the calculations is given in table 1. The aerodynamic characteristics of the Gö 711 airfoil are given in chapter 3 of KD 285 (ref. 1). The Gö 711 airfoil is only measured for $Re = 4 * 10^5$. The Reynolds values for the stations are calculated for a wind speed of 4 m/s because for most working hours, the windmill will be used at rather low wind speeds.

station	r (m)	λ_{rd} (-)	ϕ (°)	c (m)	C_{lth} (-)	C_{lin} (-)	$Re_r * 10^{-5}$ V = 4 m/s	$Re * 10^{-5}$ Gö 711	α_{th} (°)	α_{lin} (°)	β_{th} (°)	β_{lin} (°)	C_d/C_{lin} (-)
A	7.5	8	4.8	0.6	0.54	0.57	12.84	4	-1.5	-1.2	6.3	6.0	0.025
B	7.0	7.467	5.1	0.6	0.58	0.60	11.99	4	-1.1	-0.9	6.2	6.0	0.024
C	6.5	6.933	5.5	0.6	0.62	0.63	11.14	4	-0.6	-0.5	6.1	6.0	0.022
D	6.0	6.4	5.9	0.6	0.67	0.66	10.30	4	0.0	-0.1	5.9	6.0	0.021
E	5.5	5.867	6.4	0.6	0.73	0.70	9.45	4	0.7	0.4	5.7	6.0	0.020
F	5.0	5.333	7.1	0.6	0.80	0.76	8.60	4	1.6	1.1	5.5	6.0	0.019
G	4.5	4.8	7.8	0.6	0.88	0.81	7.75	4	2.6	1.8	5.2	6.0	0.017
H	4.0	4.267	8.8	0.6	0.98	0.90	6.91	4	3.8	2.8	5.0	6.0	0.015
I	3.5	3.733	10.0	0.6	1.11	1.00	6.07	4	5.6	4.0	4.4	6.0	0.015
J	3.0	3.2	11.6	0.6	1.28	1.11	5.23	4	7.7	5.6	3.9	6.0	0.017
K	2.5	2.667	13.7	0.6	1.49	1.28	4.40	4	12.0	7.7	1.7	6.0	0.020
L	2.0	2.133	16.7	0.6	1.78	1.46	3.58	4	-	10.7	-	6.0	0.028
M	1.5	1.6	21.3	0.6	2.15	1.45	2.77	4	-	15.3	-	6.0	0.094
N	1	1.067	28.8	0.6	2.58	-	2.01	4	-	22.8	-	6.0	-

table 1 Calculation of the blade geometry of the VIRYA-15 rotor

No value for α_{th} and therefore for β_{th} is found for stations L, M and N because the required C_l values can not be generated. The calculated value for β_{th} becomes smaller at smaller values of r because α_{th} is increasing faster than ϕ . The variation of the theoretical blade angle β_{th} is only little for station A up to H and varies in between 6.3° en 5.0° . Taking a constant value of 6.0° for the whole blade results in somewhat too low values for $C_{l\ lin}$ at low values of r but this is acceptable.

4 Determination of the C_p - λ and the C_q - λ curves

The determination of the C_p - λ and C_q - λ curves is given in chapter 6 of KD 35. The average C_d/C_l ratio for the outer eleven stations of the blade is about 0.02. In reality it may even be lower because the calculated Reynolds values are a lot higher than $4 * 10^5$. Figure 4.6 of KD 35 (for $B = 2$) and $\lambda_{opt} = 8$ and $C_d/C_l = 0.02$ gives $C_{p\ th} = 0.46$. The blade starts stalling somewhere in between station L and M. Therefore not the whole air foiled blade length $k = 6.5$ m, but only the part up to station L is taken into account for the calculation of the C_p . This gives an effective blade length $k' = 5.5$ m.

Substitution of $C_{p\ th} = 0.46$, $R = 7.5$ m and blade length $k = k' = 5.5$ m in formula 6.3 of KD 35 gives $C_{p\ max} = 0.427$ rounded to 0.42. $C_{q\ opt} = C_{p\ max} / \lambda_{opt} = 0.42 / 8 = 0.0525$.

Substitution of $\lambda_{opt} = \lambda_d = 8$ in formula 6.4 of KD 35 gives $\lambda_{unl} = 12.8$.

The starting torque coefficient is calculated with formula 6.12 of KD 35 which is given by:

$$C_{q\ start} = 0.75 * B * (R - \frac{1}{2}k) * C_l * c * k / \pi R^3 \quad (-) \quad (6)$$

The blade angle is 6° for the whole blade. For a non rotating rotor, the angle of attack α is therefore $90^\circ - 6^\circ = 84^\circ$. The estimated C_l - α curve for large values of α is given as figure 5.10 of KD 35 for the Gö 623 airfoil. It is assumed that this curve can also be used for the Gö 711 airfoil for large angles of α . For $\alpha = 84^\circ$ it can be read that $C_l = 0.21$. The whole blade is stalling during starting and therefore now the whole air foiled blade length $k = 6.5$ m is taken. Substitution of $B = 2$, $R = 7.5$ m, $k = 6.5$ m, $C_l = 0.21$ en $c = 0.6$ m in formula 6 gives that $C_{q\ start} = 0.0039$. For the ratio between the starting torque and the optimum torque we find that it is $0.0039 / 0.0525 = 0.074$. This is acceptable for a rotor met a design tip speed ratio of 8.

The starting wind speed V_{start} of the rotor is calculated with formula 8.6 of KD 35 which is given by:

$$V_{start} = \sqrt{\left(\frac{Q_s}{C_{q\ start} * \frac{1}{2}\rho * \pi R^3} \right)} \quad (\text{m/s}) \quad (7)$$

The sticking torque Q_s of the PM-generator is not known but it is assumed that $Q_s = 28$ Nm. Substitution of $Q_s = 28$ Nm, $C_{q\ start} = 0.0039$, $\rho = 1.2$ kg/m³ en $R = 7.5$ m in formula 7 gives that $V_{start} = 3$ m/s. This is acceptable for a 2-bladed rotor with a design tip speed ratio of 8.

In chapter 6.4 of KD 35 it is explained how rather accurate C_p - λ and C_q - λ curves can be determined if only two points of the C_p - λ curve and one point of the C_q - λ curve are known. The first part of the C_q - λ curve is determined according to KD 35 by drawing an S-shaped line which is horizontal for $\lambda = 0$.

Kragten Design developed a method with which the value of C_q for low values of λ can be determined (see report KD 97 ref. 3). With this method, it can be determined that the C_q - λ curve is about straight and horizontal for low values of λ if a Gö 623 or a Gö 711 airfoil is used. A scale model of a three bladed rotor with constant chord and blade angle and with a design tip speed ratio $\lambda_d = 6$ has been measured in the open wind tunnel of the University of Technology Delft already on 20-11-1980.

It has been found that the maximum C_p was more than 0.4 and that the C_q - λ curve for low values of λ was not horizontal but somewhat rising. This effect has been taken into account and the estimated C_p - λ and C_q - λ curves for the VIRYA-15 rotor are given in figure 1 and 2. The low C_q and C_p values at low values of λ are caused by stalling of the airfoil.

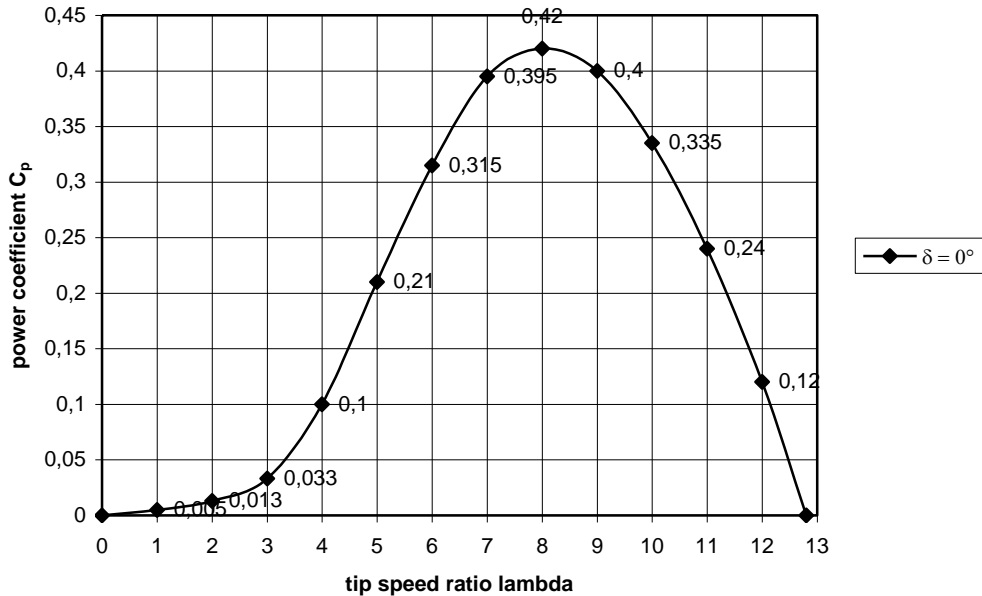


fig. 1 Estimated C_p - λ curve for the VIRYA-15 rotor for the wind direction perpendicular to the rotor ($\delta = 0^\circ$)

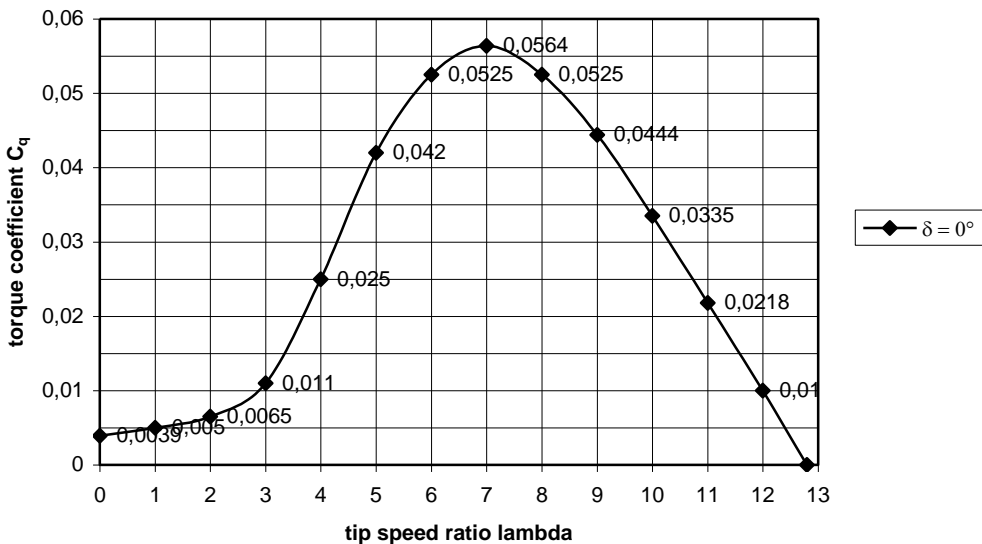


fig. 2 Estimated C_q - λ curve for the VIRYA-15 rotor for the wind direction perpendicular to the rotor ($\delta = 0^\circ$)

5 Determination of the P-n curves and the optimum cubic line

The determination of the P-n curves of a windmill rotor is described in chapter 8 of KD 35. One needs a C_p - λ curve of the rotor together with the formulas for the power P and the rotational speed n. The C_p - λ curve is given in figure 1. The VIRYA-15 has no safety system which turns the rotor out of the wind at high wind speeds like it is used for all other VIRYA windmills so it is assumed that the rotor is always perpendicular to the wind direction.

The P-n curves are used to check the matching with the P_{mech} -n curve of the generator for a certain gear ratio i. Because the P-n curve for low values of λ appears to lie very close to each other, the P-n curves are not determined for very low values of λ . The P-n curves are determined for C_p values belonging to λ is 3, 4, 5, 6, 7, 8, 9, 10, 11, 12 and 12.8 (see figure 1). The P-n curves are determined for wind the speeds 2, 3, 4, 5, 6, 7, 8, 9 and 10 m/s.

Substitution of R = 7.5 m in formula 4.8 of KD 35 gives:

$$n = 1.2732 * \lambda * V \quad (\text{rpm}) \quad (8)$$

Substitution of $\rho = 1.2 \text{ kg} / \text{m}^3$ en R = 7.5 m in formula 4.1 of KD 35 gives:

$$P = 106.029 * C_p * V^3 \quad (\text{W}) \quad (9)$$

For a certain wind speed, for instance $V = 3 \text{ m/s}$, related values of C_p and λ are substituted in formula 8 and 9 and this gives the P-n curve for that wind speed.

		V = 2 m/s		V = 3 m/s		V = 4 m/s		V = 5 m/s		V = 6 m/s		V = 7 m/s		V = 8 m/s		V = 9 m/s		V = 10 m/s	
λ	C_p	n (rpm)	P (W)	n (rpm)	P (W)														
3	0.033	7.64	28	11.46	94	15.28	224	19.10	437	22.92	756	26.74	1200	30.56	1791	34.38	2551	38.20	3499
4	0.1	10.19	85	15.28	286	20.37	679	25.46	1325	30.56	2290	35.65	3637	40.74	5429	45.84	7730	50.93	10603
5	0.21	12.73	178	19.10	601	25.46	1425	31.83	2783	38.20	4809	44.56	7637	50.93	11400	57.29	16232	63.66	22266
6	0.315	15.28	267	22.92	902	30.56	2138	38.20	4175	45.84	7214	53.47	11456	61.11	17100	68.75	24348	76.39	33399
7	0.395	17.82	335	26.74	1131	35.65	2680	44.56	5235	53.47	9046	62.39	14365	71.30	21443	80.21	30532	89.12	41881
8	0.42	20.37	356	30.56	1202	40.74	2850	50.93	5567	61.11	9619	71.30	15275	81.48	22800	91.67	32464	101.86	44532
9	0.4	22.92	339	34.38	1145	45.84	2714	57.29	5301	68.75	9161	80.21	14547	91.67	21715	103.13	30918	114.59	42412
10	0.335	25.46	284	38.20	959	50.93	2273	63.66	4440	76.39	7672	89.12	12183	101.86	18186	114.59	25894	127.32	35520
11	0.24	28.01	204	42.02	687	56.02	1629	70.03	3181	84.03	5497	98.04	8728	112.04	13029	126.05	18551	140.05	25447
12	0.12	30.56	102	45.84	344	61.11	814	76.39	1590	91.67	2748	106.95	4364	122.23	6514	137.51	9275	152.78	12723
12.8	0	32.59	0	48.89	0	65.19	0	81.48	0	97.78	0	114.08	0	130.38	0	146.67	0	162.97	0

table 2 Calculated values of n and P as a function of λ and V for the VIRYA-15 rotor

The calculated values for n and P are plotted in figure 3. The optimum cubic line which is going through the tops of the P_{mech} -n curves is also given in figure 3.

In figure 3 it can be seen that the optimum cubic line is rising very strongly for increasing wind speeds and that a very high mechanical power of 44532 W is generated at 101.86 rpm. So about 44.5 kW can be generated at a wind speed of 10 m/s. The generated electrical power depends on the efficiency of the generator η_{gen} and the inverter η_{inv} (and of the gear box if a gear box is used). Assume a direct drive PM-generator is used and that $\eta_{gen} = 0.83$ for $n = 101.86 \text{ rpm}$. Assume $\eta_{inv} = 0.95$. This gives an electrical power of about 35 kW at $V = 10 \text{ m/s}$.

The maximum power at higher wind speeds depends on the functioning of the pitch control mechanism. It will be inevitable that the absolute maximum rotational speed will be higher than 101.86 rpm because some increase of the rotational speed is required to activate the mechanism. This is because the mechanism will contain a spring with certain stiffness.

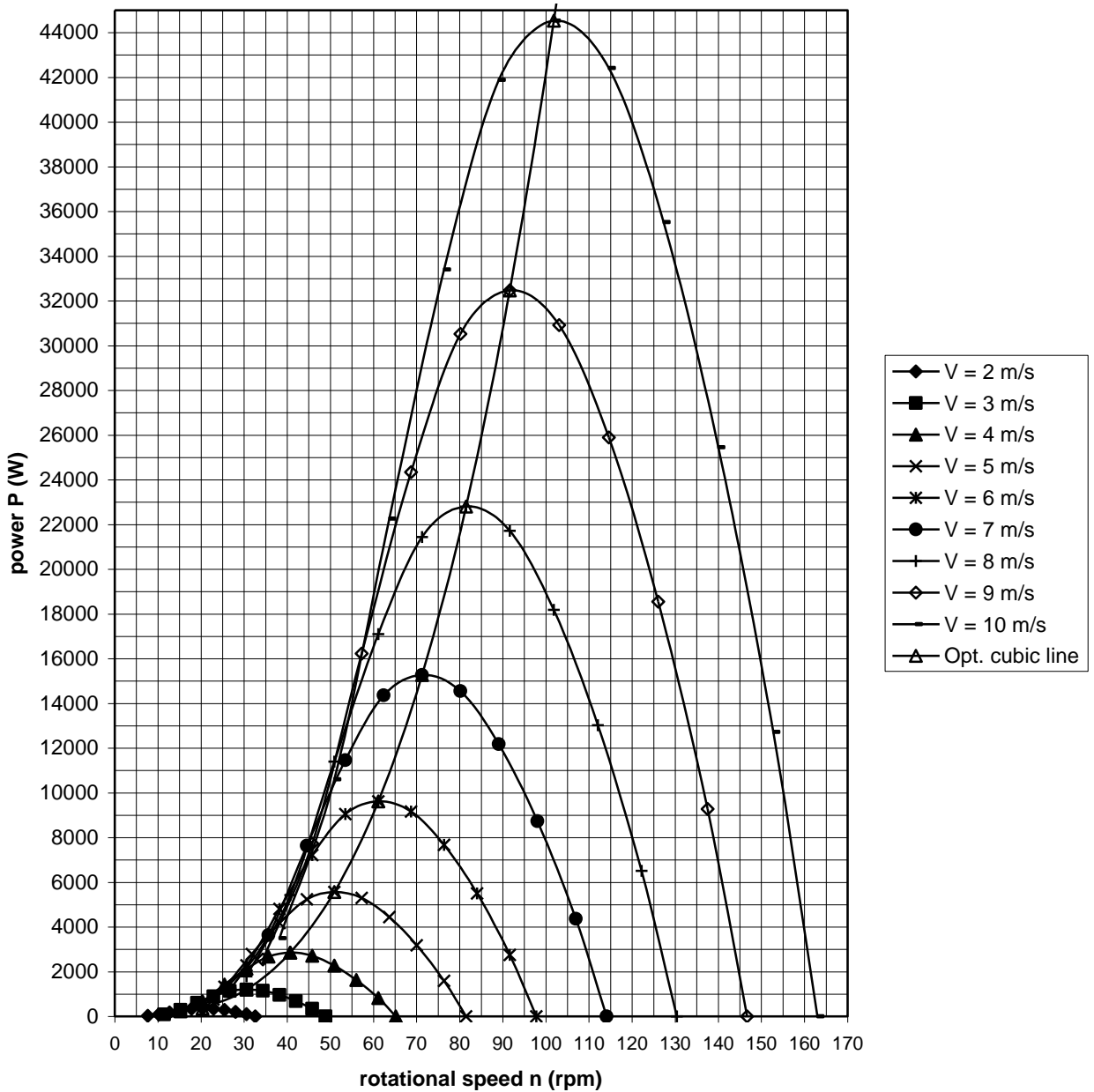


fig. 3 P-n curves and optimum cubic line of the VIRYA-15 rotor

6 General aspects of pitch control systems

The blade angle β is sometimes called the pitch angle. So a pitch control system is a safety system which uses variation of the blade angle to limit the maximum rotational speed and the maximum power. The limitation can be realised by two directions of blade rotation. Rotation of the blade to smaller blade angles is called negative pitch control or active stall. Rotation of the blade to larger blade angles is called positive pitch control.

Rotation of the blade to smaller blade angles results in increase of the angle of attack α . At a certain value of α , the maximum lift coefficient $C_{1\max}$ is reached and this is the angle α_{st} where stalling starts. For higher angles α , and so for smaller angles β , C_1 decreases somewhat but the drag coefficient C_d increases strongly if α is higher than α_{st} . At a certain angle β , the component of the drag opposed to the direction of rotation will become larger than the component of the lift in the direction of rotation (see KD 35 figure 4.4 and formula 4.14).

This means that all generated power will be used to overcome the airfoil drag. So no mechanical power can be generated on the rotor shaft and this means that the rotor will slow down if the generator withdraws power from the rotor.

The VIRYA-15 rotor is designed with a high lift coefficient at the blade root and a low lift coefficient at the blade tip. So the stalling point will move from the inside of the blade to the outside of the blade if the blade angle is decreased.

Advantages of negative pitch control

- 1) Only a rather small maximum decrease of the blade angle (about 16° , so $\beta = -10^\circ$) is needed to realise stall for the whole blade length.
- 2) A sudden wind gust results in a sudden increase of the angle of attack α . So only a little variation in the blade angle is required to realise stalling for a large part of the blade length.
- 3) If variation of the blade angle is also used to increase the starting torque, one can go from a large blade angle at starting to a small blade angle at the normal design tip speed ratio and then to a negative blade angle at stalling, using one mechanism working in the same direction.

Disadvantages of negative pitch control

- 1) It results in increase of the rotor thrust especially at the blade tip.
- 2) A stalling blade may be rather noisy.
- 3) The aerodynamic moment is working in a direction which has a tendency to increase the blade angle. So a rather large pitch moment is needed to overpower the aerodynamic moment. If this pitch moment is supplied by centrifugal weights, rather large weights will be needed.

Rotation of the blade to larger blade angles results in decrease of the angle of attack α . A smaller angle α results in decrease of the lift coefficient and so in decrease of the generated torque. So if the generator loads the rotor with a certain torque, the rotational speed will decrease.

Advantages of positive pitch control

- 1) The aerodynamic moment works in a direction which has a tendency to increase the blade angle. So the aerodynamic moment can be used to activate the pitch control system. If the aerodynamic moment is not large enough, relative small centrifugal weights are needed to give some extra pitch moment.
- 2) This system results in decrease of the lift coefficient so in decrease of the rotor thrust and so in decrease of the forces on the tower and the foundation.
- 3) The rotor stops rotating for $\beta = 99^\circ$ ($C_l = 0$, $\alpha = -9^\circ$). So no brake is needed for $\beta = 99^\circ$.

Disadvantages of positive pitch control

- 1) A rather large increase of the blade angle of about 30° is needed to limit the rotational speed enough at very high wind speeds.
- 2) A sudden wind gust results in a sudden increase of the angle of attack α . So a large blade angle will be needed to realise a blade angle α which is small enough to compensate the wind gust.

Apart from aerodynamic forces and centrifugal forces also the force due to the weight of the blade and the centrifugal weights, is active. The direction of this force with respect to the position of the blade varies 360° during one blade rotation. This will cause some variation of the blade angle. To prevent this variation, it is necessary that the movements of all blades are synchronised by the pitch control mechanism.

Pitch variation can be steered by the aerodynamic moment, by a pitch moment which is caused by centrifugal weights or by an external energy source. Modern very large 3-bladed windmills generally use an external source and a computer for each windmill. The pitch variation of all three blades is synchronised by a system of levers on each of the blade roots. The rotor shaft is hollow and contains a pin which is connected to the blade levers. The blades can rotate more than 90° if the pin is moved front- or backwards. The movement of the pin is caused by a hydraulic cylinder which is steered by the rotational speed or by the generated power. But any signal can be used to activate the pitch control system. The system can be used to stop the rotor for a positive blade angle of about 99° . It can also be used to facilitate starting, by slowly decreasing the blade angle if the rotor is accelerating.

An important disadvantage of this system is that it only works as long as energy is available to power the hydraulic system. If this energy is directly taken from the grid, the whole system will fail if the grid falls off. So some back up power is needed. This system is expected to be too complicated and too expensive for a windmill with 15 m rotor diameter.

7 Choices made for the pitch control system of the VIRYA-15

It is expected that certain developing countries will be interested to build the VIRYA-15. But as the possibilities of manufacture in these countries will be limited, the pitch control system must be as simple and as cheap as possible. The next choices were made.

- 1 A rotor with only two blades is used. A rotor with two blades allows that both blade shafts are placed in parallel to each other and therefore the whole pitch control mechanism will be rather compact.
- 2 Positive pitch control, activated by the aerodynamic moment, will be used. So no centrifugal weights will be used like it is often done for pitch control systems of small wind turbines. The axis of the blade shaft will be chosen as close as possible to the quart chord point of the airfoil.
- 3 The blade shaft will be made of 80 mm stainless steel bar which turns in INA Permaglide plain bearings or in INA needle bearings to take the rotor thrust. The centrifugal force in the blade is rather high for a rotational speed which belongs to a wind speed of 10 m/s and this force will cause a lot of friction if a Permaglide plain thrust bearing is used. So the centrifugal force in the blade will be taken by a ball or cylinder thrust bearing.
- 4 The axis of both blade shafts will have a distance of 300 mm with respect to each other. This choice in combination with the position of the axis of the blade shaft close to the quart chord point makes that the leading edge of one blade is in line with the tailing edge of the other blade (for $\beta = 0^\circ$) and this gives the rotor a nice look.
- 5 The pitch movement starts at a wind speed of 10 m/s and it is assumed that the rotor is loaded such by the generator, that it runs at $\lambda_d = 8$.
- 6 The blade can rotate over 30° , so the maximum blade angle will be 36° . It is expected that $\beta = 36^\circ$ results in a reduction of the tip speed ratio which is enough to effectively limit the rotational speed of the rotor, even for very high wind speeds.

The outer 600 mm of the blade shaft will be flattened on the side where it is connected to the blade. The blade will be clamped in between two 6 mm thick stainless steel strips and will be connected to the blade shaft by three M24 * 220 mm bolts. The blade shaft will be connected to the front side of the blade as close as possible to the quart chord point. A sketch of the connection of blade and shaft is given in figure 4.

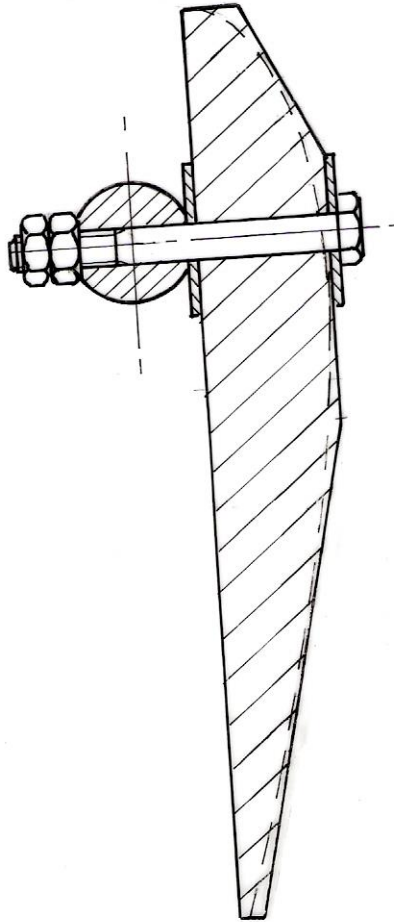


fig. 4 Connection of the blade to the blade shaft

8 Determination of the aerodynamic moment

The aerodynamic moment M depends on the aerodynamic moment coefficient C_m , the blade dimensions and the relative wind speed W which is felt by the blade. The $C_{m0.25}-\alpha$ curve of the Gö 711 airfoil is given in figure 6 of report KD 285 (ref. 1). The moment coefficient is given around the quart chord point and is therefore indicated as $C_{m0.25}$. In figure 6 of KD 285 it can be seen that $C_{m0.25}$ is almost constant for $-4^\circ < \alpha < 12^\circ$. This is favourable because it simplifies the calculation of M and the system will be rather stable. However, because of the chosen blade connection, it is not possible that the blade axis coincides with the quart chord point. Formula 1 of KD 285 gives the formula to calculate C_{mh} around a certain point H . This formula is copied as:

$$C_{mh} = C_{m0.25} + p/c \{ C_l \cos(\alpha + \gamma) + C_d \sin(\alpha + \gamma) \} \quad (-) \quad (10)$$

The blade axis is chosen as close as possible to the quart chord point which results in $\gamma = 90^\circ$. For the distance p we find that $p = 41$ mm for the chosen blade connection. The blade chord $c = 0.6$ m = 600 mm. Substitution of these values in formula 10 gives:

$$C_{mh} = C_{m0.25} + 0.0683 \{C_l \cos(\alpha + 90^\circ) + C_d \sin(\alpha + 90^\circ)\} \quad (-) \quad (11)$$

The C_l , C_d and $C_{m0.25}$ coefficients as a function of α are given in table 2 of KD 285. This table is copied as table 3.

α (°)	C_l (-)	C_d (-)	$C_{m0.25}$ (-)	$\alpha + 90^\circ$ (°)	$C_l \cos(\alpha + 90^\circ)$	$C_d \sin(\alpha + 90^\circ)$	C_{mh} (-)
-14.1	-0.173	0.1640	-0.0174	75.9	-0.0421	0.1591	-0.0094
-11.6	-0.083	0.1275	-0.0350	78.4	-0.0167	0.1249	-0.0276
-9.0	0.009	0.0928	-0.0554	81.0	0.0014	0.0917	-0.0490
-6.2	0.070	0.0587	-0.0912	83.8	0.0076	0.0584	-0.0867
-4.2	0.284	0.0299	-0.1236	85.8	0.0208	0.0298	-0.1201
-2.2	0.483	0.0165	-0.1174	87.8	0.0185	0.0165	-0.1150
0.0	0.665	0.0142	-0.1145	90.0	0	0.0142	-0.1135
2.1	0.843	0.0134	-0.1089	92.1	-0.0309	0.0134	-0.1101
4.3	1.019	0.0153	-0.1070	94.3	-0.0764	0.0153	-0.1112
6.6	1.190	0.0235	-0.1060	96.6	-0.1368	0.0233	-0.1137
8.8	1.361	0.0297	-0.1061	98.8	-0.2082	0.0294	-0.1183
11.3	1.479	0.0476	-0.1110	101.3	-0.2898	0.0467	-0.1276
14.3	1.478	0.1078	-0.1270	104.3	-0.3651	0.1045	-0.1448
17.8	1.354	0.2090	-0.1460	107.8	-0.4139	0.1990	-0.1607

table 3 C_l , C_d , C_m and C_{mh} as a function of α for $Re = 4 * 10^5$

A column for $\alpha + 90^\circ$, for $C_l \cos(\alpha + 90^\circ)$, for $C_d \sin(\alpha + 90^\circ)$ and for C_{mh} , which can be found using formula 11, is added to table 3.

Figure 6 of report KD 285 is now copied as figure 5. The calculated C_{mh} - α curve is added to figure 5. It can be seen that both curves differ only slightly. In figure 5 it can be seen that C_{mh} is about -0.115 for $-4^\circ < \alpha < 10^\circ$. The moment coefficient is defined positive if it is clockwise. So a negative moment coefficient means that the really generated aerodynamic moment has an anti clockwise direction. This means that C_{mh} has a tendency to decrease the angle of attack α and so to increase the blade angle β . Therefore it supports a positive pitch control system.

If the columns for $C_l \cos(\alpha + 90^\circ)$ and $C_d \sin(\alpha + 90^\circ)$ are observed, it can be seen that $C_d \sin(\alpha + 90^\circ)$ is always positive but it has a minimum for $\alpha = 2.1^\circ$. $C_l \cos(\alpha + 90^\circ)$ is negative for very negative angles of α , it is positive for $-9^\circ < \alpha < 0^\circ$ and negative again for $0^\circ < \alpha$. The final contribution of C_l and C_d to C_{mh} is such that the C_{mh} - α curve is lying higher than the $C_{m0.25}$ - α curve for about $\alpha < 0^\circ$ and that the C_{mh} - α curve is lying lower than the $C_{m0.25}$ - α curve for about $\alpha > 0^\circ$.

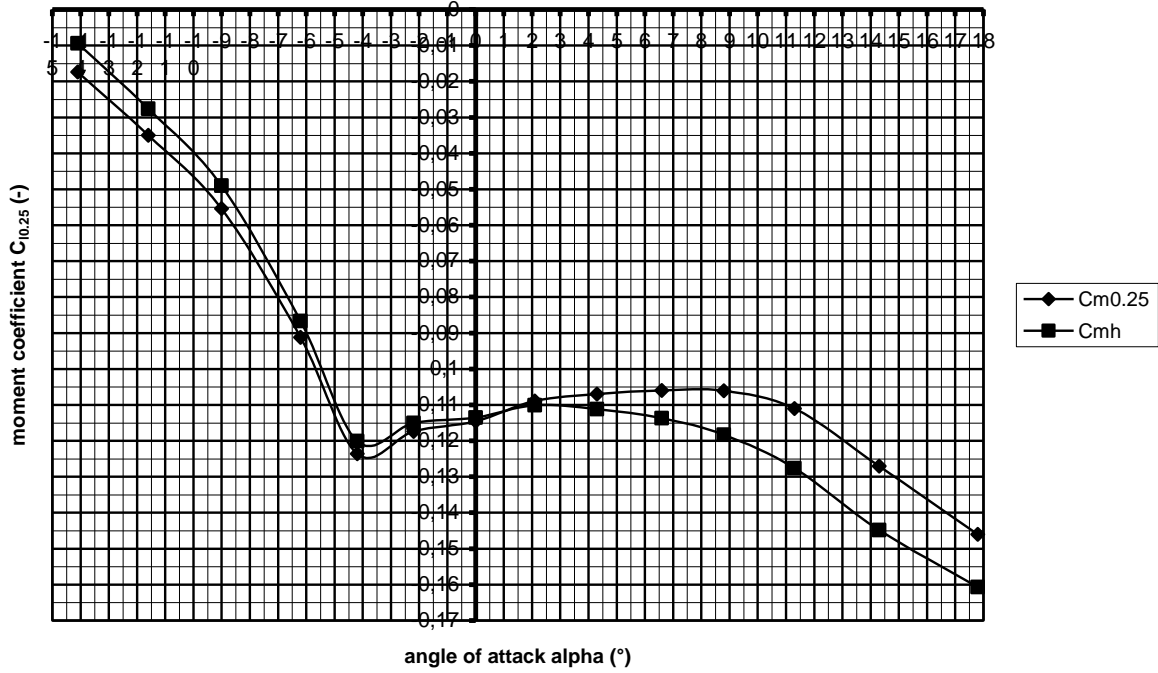


fig. 5 $C_{m0.25}-\alpha$ and $C_{mh}-\alpha$ curve for Gö 711 airfoil for $Re = 4 * 10^5$

The aerodynamic moment around point H, M_h is given by:

$$M_h = C_{mh} * \frac{1}{2}\rho V^2 * c^2 * b \quad (\text{Nm}) \quad (12)$$

In this formula, b is the airfoil width. Formula 12 is only valid if the airfoil is streamed by a wind speed V which is the same for the whole airfoil width. This is not the case for a rotating windmill blade. In this case the relative wind speed W , which is felt by the blade, differs for each station. If the wake rotation is neglected, W is given by formula 5.12 of KD 35. This formula is copied as formula 13.

$$W = V \sqrt{(\lambda_{rd}^2 + 4/9)} \quad (\text{m/s}) \quad (13)$$

Next the blade is divided into six sections 1 to 6 starting at the blade tip and each having a width $b = 1$ m. The relative wind speed is calculated for the middle of a section and it is assumed that this wind speed can be used for the whole section. The 0.5 m width section in between station M and N is neglected. The values of λ_{rd} for a certain value of r can be derived from table 1. It is assumed that the rotor is loaded such by the generator that it runs at the design tip speed ratio $\lambda_d = 8$. So the hart of section 1 corresponds to station B with $r = 7$ m and $\lambda_{rd} = 7.467$. The six sections and corresponding values of r and λ_{rd} are given in table 4.

Section	r (m)	λ_{rd} (-)	W (m/s) for $V = 10$ m/s	M_{hs} (Nm)
1	7.0	7.467	74.97	-139.6
2	6.0	6.4	64.35	-102.9
3	5.0	5.333	53.75	-71.8
4	4.0	4.267	43.19	-46.3
5	3.0	3.2	32.69	-26.5
6	2.0	2.133	22.35	-12.4

table 4 r , λ_{rd} , W and M_{hs} as a function of the section number

W is calculated for a wind speed $V = 10$ m/s. Substitution of $V = 10$ m/s in formula 13 gives:

$$W = 10 \sqrt{(\lambda_{rd}^2 + 4/9)} \quad (\text{m/s}) \quad (\text{for } V = 10 \text{ m/s}) \quad (14)$$

The calculated values of W are also given in table 4. The angle of attack α_{lin} varies in between -0.9° for section 1 with $r = 7$ m and 10.7° for section 6 with $r = 2$ m (see table 1). It is assumed that a constant value $C_{mh} = -0.115$ can be used for all six sections. Substitution of $M_h = M_{hs}$ (M_{hs} is the contribution of a section), $C_{mh} = -0.115$, $\rho = 1.2 \text{ kg/m}^3$, $V = W$, $c = 0.6$ m and $b = 1$ m in formula 12 gives:

$$M_{hs} = -0.02484 * W^2 \quad (\text{Nm}) \quad (\text{for } V = 10 \text{ m/s}) \quad (15)$$

Next M_{hs} is calculated for the values of W given in table 4 using formula 15. The calculated values of M_{hs} are also given in table 4. The total moment $M_{hs \text{ tot}}$ is the sum of all calculated values of M_{hs} .

$$\text{So } M_{hs \text{ tot}} = \Sigma M_{hs} \quad (\text{Nm}) \quad (\text{for } V = 10 \text{ m/s}) \quad (16)$$

$$\text{So } M_{hs \text{ tot}} = -139.6 -102.9 -71.8 -46.3 -26.5 -12.4 = -399.5 \text{ Nm}$$

The calculated value of M_{hs} for section 1 will be too high because of tip losses, so it is assumed that $M_{hs \text{ tot}} = -360$ Nm for $V = 10$ m/s and $\lambda_d = 8$.

$M_{hs \text{ tot}}$ is negative because the clockwise aerodynamic moment is defined positive. This is not logic for the description of the pitch movement. So from now on, the anti clockwise aerodynamic moment is defined positive and this results in a positive value of C_m and $M_{hs \text{ tot}}$. So $M_{hs \text{ tot}} = 360$ Nm and $M_{hs \text{ tot}}$ results in increase of the blade angle β .

9 Description of the synchronisation mechanism

Both blades are connected to a synchronisation mechanism which guaranties that both blades turn with the same angle. This mechanism also contains a spring and two stops, one for the standard blade angle $\beta = 6^\circ$ and one for the maximum blade angle $\beta = 36^\circ$.

The synchronisation mechanism is built in a rectangular box. The bottom of the box is connected to the generator hub. It is assumed that the rotor is positioned with the blades horizontal. The left and the right side of the box contain each two INA Permaglide bearings or INA needle bearings in which the blades can turn. Both blade axis are lying in a plane which is parallel to the bottom of the box. The bearing close to the blade foot has an inside diameter of 80 mm. The other bearing has an inside diameter of 50 mm. The box has upper and lower sides to make it very rigid. The front side of the box is closed by a cover, so the whole synchronisation mechanism is protected against weather influences.

A lever is connected to each blade shaft, just in the middle of the box. The lever has a square inside hole to connect it to a square part of the blade shaft. The lever is parallel to the bottom of the box for $\beta = 21^\circ$. The anti clockwise angle in between the lever and the bottom of the box is called χ and $\chi = 0^\circ$ for $\beta = 21^\circ$. So the relation in between χ and β is given by:

$$\chi = \beta - 21^\circ \quad (^\circ) \quad (17)$$

The end of a lever is connected to a central stainless steel pin which can move front- and backwards. For the connection a short strip is used as the pin is not able to follow the circular movement of the end of the lever. A sketch of the synchronisation mechanism is given in figure 7.

The central pin is guided in a bearing housing which is connected to the bottom of the box by two studs which are positioned in between the blade shafts. The bearing housing of the pin contains two INA Permaglide bearings. The front side of the pin is provided with a disk. A heavy compression spring is placed in between this disk and the foot of the bearing housing. The central pin and the bearing housing are designed such that the pin has a stop for $\chi = -15^\circ$ and a stop for $\chi = 15^\circ$ corresponding to respectively $\beta = 6^\circ$ and $\beta = 36^\circ$.

The reason why it is chosen that $\chi = 0^\circ$ for $\beta = 21^\circ$ is that the moment produced by a certain horizontal force on the end of a lever varies according to a cosine and that the fluctuation is only little in between $\chi = -15^\circ$ and $\chi = 15^\circ$. The horizontal force acting on the end of one lever is called F. The arm of the lever is called r_1 . So the moment M_F which is caused by F is given by:

$$M_F = F * r_1 * \cos \chi \quad (\text{Nm}) \quad (18)$$

The levers of both blades are connected to one central pin and the required horizontal force of both blades is supplied by one compression spring. So the force in the spring F_s is double the value of F which results in:

$$F = 0.5 F_s \quad (\text{N}) \quad (19)$$

(18) + (19) gives:

$$M_F = 0.5 F_s * r_1 * \cos \chi \quad (\text{Nm}) \quad (20)$$

For a wind speed $V = 10$ m/s the blade just starts to move which means that there must be balance of moments in between $M_{hs\ tot}$ and M_F . This gives:

$$0.5 F_s * r_1 * \cos \chi = M_{hs\ tot} \quad (\text{for } V = 10 \text{ m/s}) \quad (21)$$

Formula 21 can be written as:

$$F_s = 2 M_{hs\ tot} / (r_1 * \cos \chi) \quad (\text{N}) \quad (22)$$

The lever can have a maximum arm of about $r_1 = 120$ mm = 0.12 m otherwise both levers will touch each other. Substitution of $M_{hs\ tot} = 360$ Nm, $r_1 = 0.12$ m and $\chi = -15^\circ$ in formula 22 gives $F_s = 6212$ N. This requires a rather heavy compression spring.

The spring force is not constant but depends on the spring stiffness. The spring stiffness depends on the spring geometry and the required displacement s of the central pin. The displacement s of the pin from $\chi = 0^\circ$ is given by:

$$s = r_1 * \sin \chi \quad (\text{m}) \quad (23)$$

Substitution of $r_1 = 0.12$ m and $\chi = 15^\circ$ in formula 23 gives $s = 0.031$ m. The arm moves in between $\chi = -15^\circ$ and $\chi = 15^\circ$, so the total movement is $2 * s = 0.062$ m = 62 mm. The determination of the required spring geometry is out of the scope of this report.

10 Determination of the friction moment for Permaglide blade shaft bearings

A rotor blade is loaded by a bending moment which is caused by the rotor thrust or by the gyroscopic moment. As the head is turned on the wind by an electric yawing motor, the head rotation is very slowly and the gyroscopic moment can therefore be neglected. The rotor thrust F_t is given by formula 4.12 of KD 35 which is copied as formula 24.

$$F_t = C_t * \frac{1}{2} \rho V^2 * \pi R^2 \quad (\text{N}) \quad (24)$$

Formula 24 gives the rotor thrust on the whole rotor. The rotor thrust on one blade of a rotor with two blades $F_{t \text{ bl}}$ is half the value of the thrust on the whole rotor, so:

$$F_{t \text{ bl}} = 0.5 C_t * \frac{1}{2} \rho V^2 * \pi R^2 \quad (\text{N}) \quad (25)$$

The thrust coefficient for the VIRYA-15 rotor is about 0.7 if the rotor runs at $\lambda_d = 8$. Substitution of $C_t = 0.7$, $\rho = 1.2 \text{ kg/m}^3$, $V = 10 \text{ m/s}$ and $R = 7.5 \text{ m}$ in formula 25 gives that $F_{t \text{ bl}} = 3710 \text{ N}$. The distribution of the thrust over the rotor blade has about the shape of a triangle with the highest value at the blade tip. A triangle load gives a bending moment M_b at the hart of the rotor which is the same as the moment of a point load at $2/3 R$. To facilitate the calculation, it is assumed that the real thrust distribution can be replaced by a point load at $2/3 R$, so at $r_t = 5 \text{ m}$.

The blade shaft is supported in two INA Permaglide bearings. It is expected that the distance in between bearing no1 and bearing no 2 is 0.6 m. The distance a in between r_t and bearing no 1 is 4.7 m. The distance b in between r_t and bearing no 2 is 5.3 m.

The reaction force F_1 at bearing no 1 can be calculated by taking the balance of moments around bearing no 2. This gives:

$$F_1 = F_{t \text{ bl}} * b / (b - a) \quad (\text{N}) \quad (26)$$

Substitution of $F_{t \text{ bl}} = 3710 \text{ N}$, $b = 5.3 \text{ m}$ and $a = 4.7 \text{ m}$ in formula 26 gives $F_1 = 32772 \text{ N}$.

The reaction force F_2 on bearing no 2 is given by:

$$F_2 = F_1 - F_{t \text{ bl}} \quad (\text{N}) \quad (27)$$

Substitution of $F_1 = 32772 \text{ N}$ and $F_{t \text{ bl}} = 3710 \text{ N}$ in formula 27 gives $F_2 = 29062 \text{ N}$. The direction of F_1 is frontwards but the direction of F_2 is backwards. The blade will bend backwards because of the thrust and this results in a counteracting moment due to the centrifugal force in the blade. This counteracting moment reduces the bending moment in the blade but the forces F_1 and F_2 are not reduced by this effect.

Bearing no 1 has an inside diameter of 80 mm and a length of 60 mm, so the projected area $A = 80 * 60 = 4800 \text{ mm}^2$. A load of 32772 N results in a thrust pressure of 6.83 N/mm^2 which is low for a Permaglide bearing. Bearing no 2 has an inside diameter of 50 mm and a width of 60 mm, so the projected area $A = 50 * 60 = 3000 \text{ mm}^2$. A load of 29062 N results in a thrust pressure of 9.69 N/mm^2 which is also low.

The friction coefficient μ of Permaglide bearings depends on the thrust pressure (it increases at decreasing thrust pressure) and is about 0.12 for the calculated values. The friction moment M_f for a bearing with an inside bearing radius r_b (r_b is halve the inside bearing diameter) is given by:

$$M_f = \mu * F * r_b \quad (\text{Nm}) \quad (28)$$

Bearing no 1

Substitution of $\mu = 0.12$, $F = 32772$ N and $r_b = 40$ mm = 0.04 m in formula 28 gives $M_{f1} = 157$ Nm.

Bearing no 2

Substitution of $\mu = 0.12$, $F = 29062$ N and $r_b = 25$ mm = 0.025 m in formula 28 gives $M_{f1} = 87$ Nm.

So the total friction moment of both bearings together $M_{f\text{ tot}} = 157 + 87 = 244$ Nm.

This is a very large moment if compared to the aerodynamic moment $M_{hs\text{ tot}} = 360$ Nm so the pitch movement will have a lot of hysteresis. So it is expected that the use of INA Permaglide bearing may cause too much friction and that the system will therefore have too much hysteresis to work properly. As an alternative, the use of needle bearings will be investigated.

11 Use of needle bearings for the blade shaft

It was already decided to use a ball or roller thrust bearing to take the centrifugal force which pulls the blade outwards. If needle bearings are used to take the thrust load, it is logic to use a combined radial-axial needle bearing. To determine this bearing, the centrifugal force has to be calculated. For this calculation, the weight of the blade shaft is neglected but it is assumed that the wooden blade has a length $l = R = 7.5$ m. The cross sectional area A_a of a Gö 711 airfoil is about given by:

$$A_a = 0.7 * 0.1485 * c^2 \quad (\text{m}^2) \quad (29)$$

Substitution of $c = 0.6$ m in formula 29 gives $A_a = 0.0374$ m². The mass m of a blade with a density ρ_{bl} , an area A_a and a length R is given by:

$$m = \rho_{bl} * A_a * R \quad (\text{kg}) \quad (30)$$

The density of the blade ρ_{bl} depends of the kind of wood which is used for the blade. It is assumed that tropical hard wood is used, but not a heavy kind. Assume $\rho_{bl} = 0.5 * 10^3$ kg/m³. Substitution of $\rho_{bl} = 0.5 * 10^3$ kg/m³, $A = 0.0374$ m² and $R = 7.5$ m in formula 30 gives $m = 140$ kg.

The centrifugal force F_c is acting on the centre of gravity which is lying at the middle of the blade at $r_z = 3.75$ m. F_c is given by:

$$F_c = m * r_z * \Omega^2 \quad (\text{N}) \quad (31)$$

The relation in between λ , Ω , R , and V is given by formula 1.5 of KD 35. This formula can be written as:

$$\Omega = \lambda * V / R \quad (32)$$

Substitution of $\lambda = \lambda_d = 8$, $V = 10$ m/s and $R = 7.5$ m in formula 32 gives $\Omega = 10.667$ rad/s. Substitution of $m = 140$ kg, $r_z = 3.75$ m and $\Omega = 10.667$ rad/s in formula 31 gives $F_c = 59737$ N. Assume $F_c = 60000$ N.

The combined radial-axial bearing can be positioned at bearing no 1 or at bearing no 2. Positioning at bearing no 1 has the advantage that the thrust bearing is in the box. However, combined radial-axial bearings are not available with an inside diameter of 80 mm. So the combined radial axial bearing has to be positioned at bearing no 2.

Combined radial-axial bearings are available with a ball thrust bearing or with a cylinder thrust bearing. The static load factor C_0 for a cylinder thrust bearing is much higher than for a ball thrust bearing so a cylinder thrust bearing is selected. The largest size of a combined radial-axial bearing with a cylinder thrust bearing has an inside diameter of 50 mm. The type with dust cap has INA code NKXR 50 Z and this type is chosen for bearing no 2.

The bearing will make only very slow movements and therefore the bearing has to be calculated for static load conditions. The static axial load factor of bearing NKXR 50 Z is 177000 N which is certainly enough for a centrifugal force of 60000 N.

The radial load for bearing no 2 was calculated in chapter 10 and it was found that $F_2 = 29062$ N. The static radial load factor of bearing NKXR 50 Z is 74000 N so this is certainly enough for a radial force of 29062 N.

Bearing NKXR 50 Z is supplied without an inner ring. The bearing can't run directly on the stainless steel blade shaft because this material is not hard enough. So an inner ring type IR 45 * 50 * 25 is selected. This means that the shaft at bearing no 2 will have a diameter of 45 mm. At this shaft end, a heavy disk is connected with a heavy M30 bolt and this disk transforms the centrifugal force to the thrust bearing. The thrust bearing is mounted at the outside of the box and a cover with a sealing in it is needed to prevent entrance of water and dust in bearing no 2.

For bearing number 1 it is also not allowed that the bearing runs directly on the stainless steel of the blade shaft. Inner rings with an inside diameter of 80 mm have an outside diameter of 90 mm. So a needle bearing with an inside diameter of 90 mm is required. The smallest bearing with this inside diameter has INA code NK 90/25 (width 25 mm).

The radial load for bearing no 1 was calculated in chapter 10 and it was found that $F_2 = 32772$ N. The static radial load factor of bearing NK 90/25 is 123000 N so this is certainly enough for a radial force of 32772 N.

The selected inner ring has INA code IR 80 * 90 * 25. It is expected that for the stainless steel shaft, a diameter of 80 mm is used but that this diameter is not accurate enough for directly pressing the inner ring to the shaft. Therefore it is assumed that the shaft is turned or ground to a diameter of 79.9 mm and that the inner ring is glued to the shaft by epoxy glue or anaerobe glue. A sealing is required to prevent entrance of water and dust in bearing no 1.

The friction coefficient for needle bearings is very low (about 0.003) so the friction moment can be neglected. An extra advantage is that needle bearings are rather short and that therefore a much thinner sheet can be used for the box sides, than for Permaglide bearings.

12 Estimation of the braking capacity of the PM-generator

It is assumed that a direct drive permanent magnet (PM) generator is used. A PM-generator can be used as a brake if the winding is short-circuited. The generator can be short-circuited in star or in delta. The maximum torque level for short-circuit in delta is higher than for short-circuit in star because in delta, higher harmonic currents can circulate in the winding. Short-circuit in star is identical to short-circuit in delta if the star point is short-circuited too. It is assumed that the generator is normally used for star rectification but that it is short-circuited in delta to get the maximum torque level. It is also assumed that the short-circuit switch is positioned before the rectifier. So to make short-circuit in delta, an extra cable is needed from the star point of the generator to the short-circuit switch.

The PM-generator is not yet selected, so the characteristics are not known. I have designed and measured many PM-generators for small VIRYA windmills, so the characteristics of the VIRYA-15 PM generator can be estimated.

The maximum torque level of a permanent magnet generator for a certain way of rectification is about constant for every voltage and so for every rotational speed. In chapter 5 it has been calculated that the maximum power of the rotor is 44532 W for $n = 101.86$ rpm. The torque Q at this rotational speed can be calculated with:

$$Q = 30 P / (\pi * n) \quad (\text{Nm}) \quad (33)$$

Substitution of $P = 44532$ W and $n = 101.86$ rpm in formula 33 gives $Q = 13116$ Nm. This is not the maximum torque level of the generator because at the maximum torque level the generator can't have a high efficiency. The maximum torque level of the generator at star rectification must be at least a factor 1.5 higher, so it must be about 20000 Nm. The maximum torque level at delta rectification will be about a factor 1.25 higher than for star rectification, so it will be about 25000 Nm. This maximum torque will be supplied at a very low rotational speed of about 30 rpm if the generator is short-circuited. An estimated Q - n curve of the PM-generator for short circuit in delta is given in figure 6.

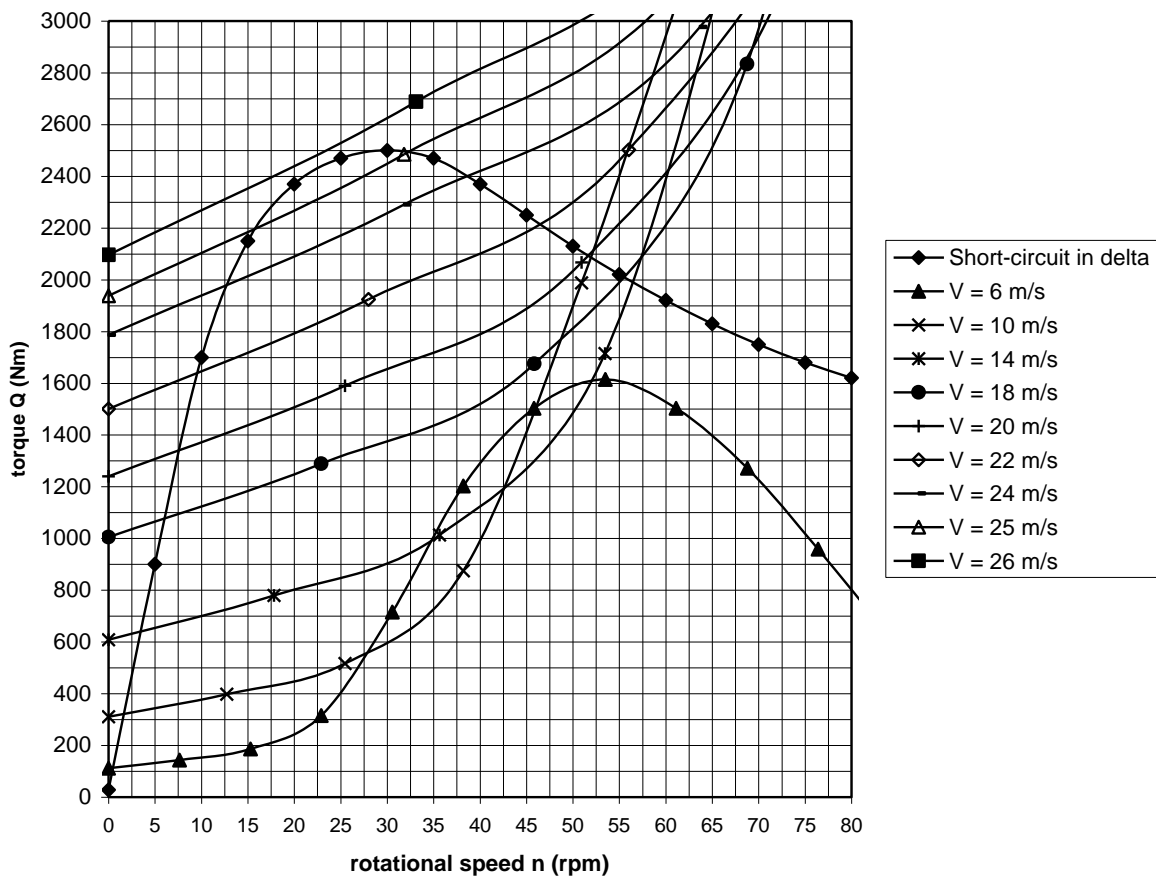


fig. 6 Estimated Q - n curve of the PM-generator for short-circuit in delta and Q - n curves of the rotor for high wind speeds

The Q - n curves of the rotor for high wind speeds can be derived in the same way as the P - n curves of figure 3 but one has to use the formula for Q in stead of the formula for P . The formula for Q is given as formula 4.3 in KD 35. Substitution of $\rho = 1.2$ kg/m³ and $R = 7.5$ m in formula 4.3 of KD 35 gives:

$$Q = 795.22 * C_q * V^2 \quad (\text{Nm}) \quad (34)$$

The rotational speed n is given by formula 8. The Q - n curves are determined for wind speeds of 6, 10, 14, 18, 20, 22, 24, 25 and 26 m/s for values of λ of 0, 1, 2, 3, 4 and 5 (see figure 2 for the C_q - λ curves). The result of the calculations is given in table 5 and figure 6.

λ	C_q	V = 6 m/s		V = 10 m/s		V = 14 m/s		V = 18 m/s		V = 20 m/s		V = 22 m/s		V = 24 m/s		V = 25 m/s		V = 26 m/s	
		n (rpm)	Q (Nm)	n (rpm)	Q (Nm)	n (rpm)	Q (Nm)	n (rpm)	Q (Nm)	n (rpm)	Q (Nm)	n (rpm)	Q (Nm)	n (rpm)	Q (Nm)	n (rpm)	Q (Nm)	n (rpm)	Q (Nm)
0	0.0039	0	111.6	0	310.1	0	607.9	0	1004.8	0	1240.5	0	1501.1	0	1786.4	0	1938.3	0	2096.5
1	0.005	7.64	143.1	12.73	397.6	17.82	779.3	22.92	1288.3	25.46	1590.4	28.01	1924.4	30.56	2290.2	31.83	2485.1	33.10	2687.8
2	0.0065	15.28	186.1	25.46	516.9	35.65	1013.1	45.84	1674.7	50.93	2067.6	56.02	2501.8	61.11	2977.3	63.66	3230.6	66.21	3494.2
3	0.011	22.92	314.9	38.20	874.7	53.47	1714.5	68.75	2834.2	76.39	3499.0	84.03	4233.8	91.67	5038.5	95.49	5467.1	99.3	5913.3
4	0.025	30.56	715.7	50.93	1988.1	71.30	3896.6	91.67	6441.3	101.86	7952.2	112.04	9622.2	122.23	11451	127.32	12425	132.4	13439
5	0.042	38.20	1202.4	63.66	3339.9	89.12	6546.3	114.59	10821	127.32	13360	140.05	16165	152.78	19238	159.15	20875	165.52	22578

table 5 Calculated values of n and Q as a function of λ and V for the VIRYA-15 rotor

The left point of intersection of the estimated Q - n curve of the PM-generator for short circuit in delta with the Q - n curve of the rotor for a certain wind speed gives a stable working point for that wind speed. The right point of intersection gives an unstable working point because the rotor torque increases faster than the generator torque at increasing rotational speed. So the rotor can only be stopped for combinations of Q and n which are lying lower than the Q - n curve of the generator for short-circuit in delta.

In figure 6 it can be seen that there is no point of intersection for a wind speed of 26 m/s which means that the rotor will start rotating from stand still position even if the generator is short-circuited. When this happens the generator will burn within some minutes because all generated power will be transformed into heat!

Figure 6 gives no direct indication below which wind speed the rotor can be stopped when it is rotating! It was assumed that the generator is loading the rotor such that the rotor is following the optimum cubic line. In figure 3 it can be seen that the rotor is running at more than 100 rpm for a wind speed of 10 m/s. So this rotational speed is lying far right from the unstable working point for $V = 10$ m/s which lies about at $n = 52$ rpm.

The Q - n curve of the rotor for $V = 6$ m/s has also been drawn for higher values of λ . It can be seen that this curve is lying lower than the Q - n curve of the generator for short-circuit in delta. So the rotor can be stopped for this wind speed (and for lower wind speeds). But the Q - n curve for $V = 7$ m/s (not drawn) will already have two points of intersection with the Q - n curve of the generator, so the rotor can certainly not be stopped for higher wind speeds.

So it is advised if one wants to stop the rotor, that the rotor is first turned out of the wind a lot which will result in a strong reduction of the rotational speed. Only if the rotational speed is below about 30 rpm, where the braking torque is maximal, the generator can be short-circuited.

For the determination of the Q - n curves of the rotor, the C_q - λ curve of figure 2 is used. This C_q - λ curve is valid for a blade angle $\beta = 6^\circ$. Increase of the blade angle will result in a strong increase of the C_q - λ curve for low values of λ . So it has to be investigated how the safety mechanism functions for very high wind speeds if the rotor runs at a very low tip speed ratio. Assume the generator is short-circuited and the rotor is perpendicular to the wind and $V = 25$ m/s. In figure 6 it can be seen that the stable working point is lying at a rotational speed of about 15 rpm. The tip speed ratio λ is about 0.5 for this rotational speed. The local speed ratio λ_r decreases about linear with r so at $r = 3.75$ it is only about 0.25. There is only a little difference in between the angles of attack for a rotor which is running very slowly and a rotor which is stopped completely, so it is assumed that the rotor is stopped completely. This means that the angle of attack is $90^\circ - 6^\circ = 84^\circ$ for the whole blade. For this large angle, the lift is only little but the drag is very large. The moment coefficient for the Gö 711 airfoil is not given for very large angles α but the moment is almost complete produced by the drag. It is assumed that the point of exertion of the drag is lying about at the hart of the blade. So the distance r_e in between the point of exertion and the quart chord point is about 0.25 c .

The drag coefficient for the Gö 711 is also not given for very large angles α but it is expected that it is almost the same as for the Gö 623 airfoil for which it is about 2 for $\alpha = 84^\circ$. However, this is only true for a blade with an infinite aspect ratio. Because of tip losses the average drag coefficient will be lower and it is assumed that it is about 1.8. The pitch moment M for a total blade length $b = 7.1$ m is now given by:

$$M = 0.25 c * C_d * \frac{1}{2} \rho V^2 * c * b \quad \text{or}$$

$$M = 0.125 * C_d * \rho V^2 * c^2 * b \quad (\text{Nm}) \quad (35)$$

The blade starts turning around the blade axis when M is equal to the moment which is produced by the spring of the pitch control mechanism. In chapter 8 it was calculated that this moment $M_{hs \text{ tot}} = 360$ Nm. The critical wind speed V_{crit} at which the blade starts turning around the blade axis can now be calculated with:

$$V_{crit} = \sqrt{\{8 M_{hs \text{ tot}} / (C_d * \rho * c^2 * b)\}} \quad (\text{m/s}) \quad (36)$$

Substitution of $M_{hs \text{ tot}} = 360$ Nm, $C_d = 1.8$, $\rho = 1.2$ kg/m³, $c = 0.6$ m and $b = 7.1$ m in formula 36 gives $V_{crit} = 22.8$ m/s. This means that the blade will turn to larger blade angles for wind speeds larger than 22.8 m/s and for this situation the C_q - λ curve of figure 2 can no longer be used. This means that only the curves for $V = 22$ m/s and lower out of figure 6 are correct! So the rotor must certainly be turned out of the wind for wind speeds higher than 22.8 m/s.

Another reason why it might be necessary that a stopped rotor has to be turned out of the wind at very high wind speeds is that the rotor may be not strong enough to resist the very high bending moment which will happen in the blade foot. The calculation of the rotor geometry as given in chapter 3 gives only the geometry of a rotor with a constant chord blade for a design tip speed ratio of 8. It tells nothing about the strength of the rotor blades.

13 Functioning of the system for $V > 10$ m/s

Exact description of the functioning of the system at wind speeds higher than 10 m/s is very difficult for several reasons.

The first reason is that the C_p - λ and C_q - λ curves will change at larger blade angles β . For a larger β and the same chord c , the rotor is no longer designed according to the aerodynamic theory as used in chapter 3. A larger blade angle results in a lower optimum tip speed ratio λ_{opt} and for a lower value of λ_{opt} , the blade chord for an optimum design should be much larger. As the blade chord doesn't change, this means that the rotor is no longer able to reduce the wind speed in the rotor plane up to 2/3 of the undisturbed wind speed V , what is a criteria for the aerodynamic theory. For large blade angles β , the rotor will get a very low value of λ_{opt} but in this case the angle ϕ in between the direction of the relative wind W and the rotor plane will increase strongly at decreasing radius r . This means that a rotor with no blade twist will be streamed at large negative angles of attack α at the blade tip but at large positive angles α at the blade root. So the simple method to determine C_p - λ and C_q - λ curves, as given in chapter 4, can no longer be used.

The second reason is that without selecting a certain compression spring for the synchronisation mechanism, it is not known how $M_{hs \text{ tot}}$ will vary as a function of the angle χ in between the blade lever and the bottom of the box. For the time being it is assumed that the mechanism is designed such that $M_{hs \text{ tot}}$ increases only slightly for 30° blade rotation. This means that a long spring will be required.

The third reason is that the wind speed can vary differently above $V = 10$ m/s. It can increase slowly or very suddenly.

So only a general description can be given. The system will react differently on wind speed variations above 10 m/s.

Assume the wind speed increases very suddenly from 10 m/s up to 15 m/s. This means that the tip speed ratio, suddenly decreases from 8 to $8 * 10/15 = 5.33$. This results in a strong increase of the angle of attack α for all blade stations. For the outer stations this will not result in strong variation of the moment coefficient C_{mh} because the normal angles α are very small (see table 1 and figure 5). However, for the inner stations which are normally streamed under rather large angles α , sudden increase of α will result in very large values of α . For very large values of α it is no longer allowed to assume that C_{mh} is about constant and has a value of -0.115. In figure 5 it can be seen that e.g. $C_{mh} = -0.1607$ for $\alpha = 18^\circ$.

In table 4 it can be seen that the contribution of the inner blade sections to M_{hs} is not very important but they can't be neglected. A sudden wind gust will therefore immediately result in some increase of $M_{hs\ tot}$ and this will result in a direct increase of β . This increase of β results in decrease of the optimum tip speed ratio λ_{opt} and in decrease of the maximum power coefficient $C_{p\ max}$ which is realised at that lower value of λ_{opt} .

The second effect of the increase of the angle of attack α is that the component of the lift in the direction of rotation increases and this will result in acceleration of the rotor, so in increase of the tip speed U and therefore also in increase of the relative wind speed W . Formula 15 shows that M_{hs} increase proportional to W^2 , so some increase of the rotational speed of the rotor has a relatively large influence on M_{hs} . So only a small increase of the rotational speed will result in a rather large increase of the angle β . This second effect is the main reason why this safety system is very sensible and why only a little increase of the rotational speed is needed to sufficiently reduce the tip speed ratio at high wind speeds.

The second effect is the only effect which is working if the wind speed increases only slowly above $V = 10$ m/s.

14 References

- 1 Kragten A. The Gö 711 airfoil for use in windmill rotor blades, June 2006, free public report KD 285, engineering office Kragten Design, Populierenlaan 51, 5492 SG Sint-Oedenrode, The Netherlands.
- 2 Kragten A. Rotor design and matching for horizontal axis wind turbines, July 2004, free public rapport KD 35, engineering office Kragten Design, Populierenlaan 51, 5492 SG Sint-Oedenrode, The Netherlands.
- 3 Kragten A. Determination of C_q for low values of λ . Deriving the C_p - λ and C_q - λ curves of the VIRYA-1.8D rotor, July 2002, free public rapport KD 97, engineering office Kragten Design, Populierenlaan 51, 5492 SG Sint-Oedenrode, The Netherlands.

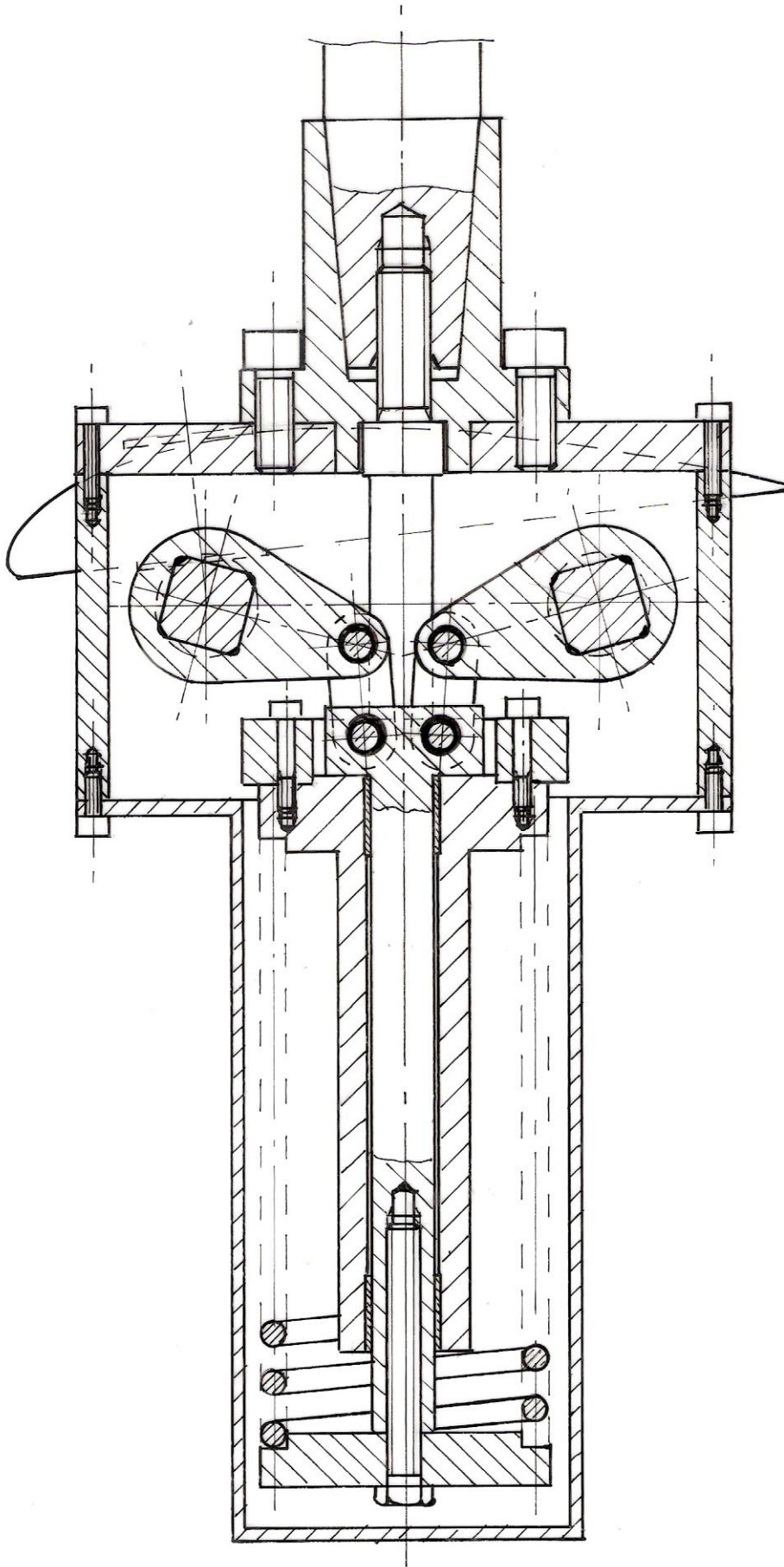


fig. 7 Sketch of the synchronisation mechanism